PhD Candidacy Proposal:

A Strategy for a Single-Photon Source Using a Kerr-Cavity Weakly Coupled to a Quantum Emitter

c praise anyanwu *

Chemistry Department, University of Washington

14 December 2022

*anyanc@uw.edu

1 Introduction

Encoding information in the quantum state of a single photon (using degrees of freedom of polarization, momentum, or energy) is highly desirable in secure quantum communication since photons travel at the speed of light and interact weakly with the environment over long distances. [1, 2] For example, in the quantum key distribution protocol, Alice encodes information in the qubit of a photon polarization state. [3, 4] Importantly, if Alice must securely transmit this qubit through a quantum channel to Bob, and without loss of information to an eavesdropper, then Alice's single-photon source must be deterministic. A deterministic single-photon source emits a single photon *on demand*, with 100 % probability. In practice, one evaluates the single-photon nature of a source by the ratio of the probability of single-photon to multi-photon emission. [5, 6]

Deterministic single-photon sources involve effective two level systems (quantum dots, single atoms, single ions) [7, 8, 9, 10, 11] that emit a single photon when excited by a resonant incident field. Less deterministic single-photon sources involve nonlinear processes as parametric down conversion in waveguides (or four-wave mixing in optical fiber systems) [12, 13, 14] that emit a correlated pair of photons, where one photon heralds the other. The known difficulties with these systems involve trapping of a single ion or atom strongly coupled to cavities at cryogenic temperatures for deterministic single-photon sources, while care must be taken for less deterministic sources

in order to avoid generating multiple pairs of photons. Herein, we propose a theoretical basis for a novel single-photon source that circumvents both ion-trapping at ultra-cold temperatures and the need for strong coupling. The measure of the system's single-photon nature is based on the calculated second order correlation function of transmitted light.

Consider the following system: a high-Q cavity coupled to a broad-band emitter. For example, ref. [15] has an emitter placed on the chip of a toroidal silica microcavity with a 10^7 Q-factor (Fig. 1a). We propose the following modification: a quantum emitter placed on a Kerr-cavity coated with polystyrene, which has a significant 10^{-12} cm^2/W third-order nonlinear susceptibility. [16, 17] (Polystyrene's third-order nonlinearity originates from the delocalization of the π-conjugated electrons along the polymer chains. [18, 19]) This achieves a Kerr effect such that the resonance of the nonlinear cavity now depends on the photon-number in the cavity (Fig. 1b).

A characteristic of the coupled Kerr-cavity-emitter system is the cavity photon-number dependent Fano resonance, with a resonant peak and anti-resonant dip corresponding to an enhanced and diminished absorption by the emitter (see Fig. 1b). Just at the vicinity of the anti-resonance, there is transmission of a photon into the cavity. Upon single-photon population, the Kerr-cavity resonance is detuned from a pump laser exciting the system at the anti-resonance. And if the kerr-cavity resonant frequency shift is on the order Γ (the FWHM equal to the line-width between the anti-resonant dip and the resonant peak of the Fano Profile), then the system experi-

a. Simultaneous Measurement

$|\mathbf{E}_{Laser}|$
g
γ_p
γ_c
$\chi^{(3)}$

Absorption

Energy

Transmission

Energy

b.
$\omega_L = \omega_c$

$S(\omega_L)$

1.25
1.00
0.75
0.50
0.25
0

-20.02 -20.00 -19.98 -19.96

$\hbar(\omega_L - \omega_p)$ meV

$N_c = 0$
$N_c = 1$

c.

$g_{ss}^{(2)}(\omega_L = \omega_c; N_c = 1)$

0.6
0.4
0.2
0

0 1 2 3 4
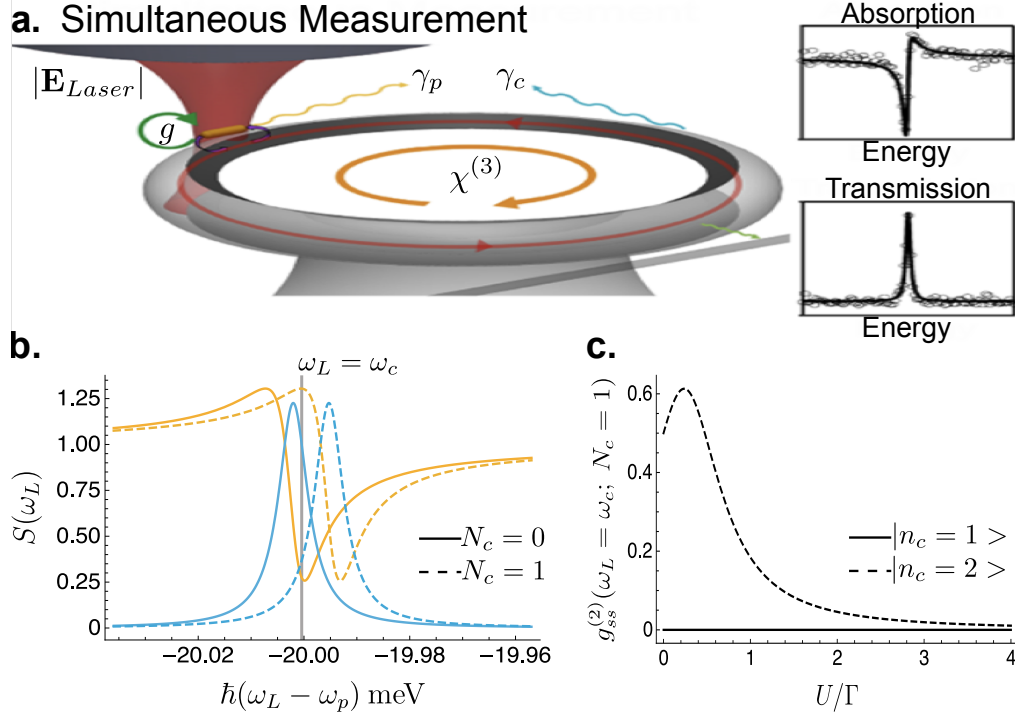
U/Γ

$|n_c = 1>$
$|n_c = 2>$

Figure 1: (a) Example of the proposed experimental set-up [15], which in general, consists of a broad-band quantum emitter (here represented as gold nanorod) placed unto—and weakly coupled to—a Kerr-cavity (here represented as toroidal micro-ring resonator). The emitter is pumped with a laser, and its absorption spectrum shows a Fano profile due to its interaction with the high-Q cavity. At the vicinity of the anti-resonance, there is a peak in transmission of light through the cavity out-coupled to the measuring fiber optic cable. (b) The spectral distribution of the reduced average photon-number in the broad-band mode at steady-state $\langle b^\dagger b \rangle_{ss}/\langle b^\dagger b \rangle_{ss;g=0}$, yellow curves, and the average photon number in the discrete cavity mode of a single-photon state $\langle n_c = 1| a^\dagger a |n_c = 1\rangle_{ss}$, blue curves. The solid curves are the spectra when the cavity has zero-photon occupation $N_c = 0$, while the dashed curves, the cavity has a single-photon occupation $N_c = 1$. (c) The second order correlation calculated at steady state when the cavity is populated with a single-photon occupation. The single-photon blockade is eviedent for a Kerr-nonlinearity whose value is withtin the order of the Fano line-width, i.e., $\chi^{(3)} \propto U = \Gamma$.

4

ences a single-photon blockade, as shown in the calculated $g_{ss}^{(2)}$ (Fig. 1c) of light transmitted through the cavity at steady state. Thus the single-photon blockade effect depends on the Fano resonance shift $\Delta\omega$ induced by the Kerr-cavity's non-linearity, where the degree of nonlinearity that induces the shift $\Delta\omega$ is proportional to Γ, such that,

$$\omega_1 - \omega_0 = (\omega_0 + \Gamma) - \omega_0$$
$$\Delta\omega = \Gamma \tag{1}$$

with $\omega_{0,1} = cn_{0,1}k$, and n_1 is the refractive index due to the kerr effect [20]:

$$n_1 = n_0 + n_2 I$$
$$= n_0 + \frac{3\chi^{(3)}}{8n_0 c\epsilon_0} I. \tag{2}$$

Note that n_2 is the value often reported for the third-order susceptibility, such that the Kerr effect is induced by the local intensity I from the pump laser populating the kerr-cavity. From the above equations we find the relation:

$$\frac{\Delta\omega}{ck} = n_2 I \tag{3}$$

For a cavity mode $\lambda \approx 1566$ nm, [15, 21] with a third-order susceptibility $n_2 \approx 1.15 \times 10^{-12}$ cm^2/W, [16] the desired blockade effect can be achieved for a single-photon state whose resonance is shifted by $\Delta\omega \approx \Gamma$, if the local intensity $I \geq 7.41$ MW/cm^2, which is the regime of a faint laser beam whose

coherent state could have an average photon-number in the range $\mu = 0.1 - 2$. [22] This is advantageous because the desired blockade effect could be achieved with a faint laser beam or with a kerr-cavity of much smaller n_2.

2 Model

We develop the system's dynamics in Heisenberg picture. Heisenberg picture is suitable to calculate the quantum statistical correlation of the field of light transmitted through the Kerr cavity. This field correlation can be related to the experimentally observed spectral distribution, using the spectral response function. [23] Moreover, in the Heisenberg picture the dynamics of the quantum transverse field is analogous to the classical transverse field [24], which allows for direct comparison to the classical system. [15] Then damping of the single-mode in the cavity field (and of the broad-band field) is described using Heisenberg-Langevin formalism. In so doing, this model provides a simple yet rigorous quantum approach (complementing the Louivillian formalism in the Linblad form, recently developed in Ref. [25, 26]) to account for damping of the discrete state (cavity mode) of Fano resonance, and the spectral distribution derived from this model is expressed in terms of Fano-parameters. [27]

The Hamiltonian of the discrete Kerr-cavity coupled to a broad-band emitter is the following: $\mathcal{H} = \mathcal{H}_a + \mathcal{H}_b + \mathcal{H}_f + \mathcal{H}_I$. The derived Hamiltonian $\mathcal{H}_a$ is the energy of a single-mode dielectric Kerr-cavity in free space [28, 29],

such that,

$$
\begin{aligned}
\mathcal{H}_a &= \frac{1}{2} \int_V \mathrm{d}^3\mathbf{x}\, \mathbf{P} \cdot \mathbf{E} \\
&= \frac{1}{2} \int_V \mathrm{d}^3\mathbf{x} \left(\mathbf{P}^{(1)} + \mathbf{P}^{(3)} \right) \cdot \mathbf{E} \\
&= \frac{1}{2} \int_V \mathrm{d}^3\mathbf{x} \left(\boldsymbol{\chi}^{(1)}\mathbf{E} + \frac{3}{4}\boldsymbol{\chi}^{(3)} : \mathbf{E}\mathbf{E}^*\mathbf{E} \right) \cdot \mathbf{E}
\end{aligned}
\tag{4}
$$

where $3/4\chi^{(3)}$ is the higher order nonlinear susceptibility of a Kerr-cavity [30], and the quantized field $\mathbf{E}$ is normalized with respect to the cavity's mode volume V. In the rotating wave approximation (and for a linear polarization), $\mathcal{H}_a$ simplifies as follows

$$
\begin{aligned}
\mathcal{H}_a &= \pi\hbar\omega_k \left(\chi_{ef}^{(1)} + \frac{3}{4}\chi_{ef}^{(3)}\mathcal{E}^2 a^\dagger a + \frac{3}{4}\boldsymbol{\chi}^{(3)}\mathcal{E}^2 : \mathbf{1} \right)\left(a^\dagger a + \frac{1}{2} \right) \\
&= \hbar\left(\omega_c + U\, a^\dagger a \right)\left(a^\dagger a + \frac{1}{2} \right) \\
&\approx \hbar\left(\omega_c + U\langle a^\dagger a\rangle \right)\left(a^\dagger a + \frac{1}{2} \right).
\end{aligned}
\tag{5}
$$

where $\mathcal{E} = \sqrt{2\pi\hbar\omega_k/V}$ is the amplitude of the quantized field.

The first-order approximation in Eq. (5) linearizes the nonlinear term. This is based on the motivation that the resonant frequency of a kerr-cavity changes as a function of intensity $|\mathbf{E}|^2$. In this case, the resonant frequency depends on the average photon-number in the Kerr-cavity:

$$
\omega_c^{NL}(N_c = \langle a^\dagger a\rangle) = \omega_c + U N_c.
\tag{6}
$$

Thus the Hamilonian for the single-mode Kerr-cavity $\mathcal{H}_a$, the bosonic broad-band field $\mathcal{H}_b$, and the free field $\mathcal{H}_f$ is as follows:

$$\mathcal{H}_a = \hbar\omega_c^{NL}\left(a^\dagger a + \frac{1}{2}\right), \tag{7}$$

$$\mathcal{H}_b = \hbar\omega_p\left(b^\dagger b + \frac{1}{2}\right), \tag{8}$$

$$\mathcal{H}_f = \hbar\sum_j \omega_j\left(f_j^\dagger f_j + \frac{1}{2}\right). \tag{9}$$

The discrete cavity mode ω_c^{NL} and the broad-band mode ω_p both disipate energy to the free fields ω_k. Thus the interaction Hamiltonian $\mathcal{H}_I$ is as follows:

$$\mathcal{H}_I = \hbar g\left(a^\dagger b + b^\dagger a\right) + \hbar\sum_j (V_j^a f_j^\dagger a + V_j^b f_j^\dagger b + \text{h.c.}). \tag{10}$$

We work in Purcell regime where $|V_a| \ll g \ll |V_b|$. Note that the original Fano problem is the limit where $|V_a| \to 0$.

Deriving the Heisenberg-Langevin equation of motion for the slowly varying operator $A = a\, e^{i\omega_c^{NL}t}$, and then transforming back to the non-slowly varying operator $a = A\, e^{-i\omega_c^{NL}t}$ yields

$$\dot{a} = -i(\omega_c^{NL} - i\gamma_c/2)a - igb, \tag{11}$$

$$\dot{b} = -i(\omega_p - i\gamma_p/2)b - iga, \tag{12}$$

$\gamma_{c,p}$ accounts for both radiative and non-radiative damping as described in Ref [31]. (Note that the above equation has assumed an evacuated initial

8

reservoir state.)

In the experiment, the broad-band mode is driven by the external field of a monochromatic laser operating at ω. The spectral distribution is derived from the spectral response function, such that,

$$S(\omega) = \frac{1}{\pi} \int_0^\infty d\tau \, e^{i\omega\tau} \langle b^\dagger(t_0 = 0) \, b(t_0 + \tau) \rangle. \tag{13}$$

We find that the spectral response function can be interpreted as the steady state solution of the average photon-number in the broad-band mode rotating in the frame of the drive frequency, i.e.

$$S(\omega) = \langle \tilde{b}_{ss}^\dagger \tilde{b}_{ss} \rangle \tag{14}$$

$$\tilde{b}_{ss}^\dagger = b_{ss}^\dagger \, e^{i\omega_L t}; \quad \tilde{a}_{ss}^\dagger = a_{ss}^\dagger \, e^{i\omega_L t}; \tag{15}$$

$$\dot{b}_{ss} = 0 = -i(\omega_p - i\gamma_p/2)b_{ss} - iga_{ss} + iE_{Laser}(e^{i\omega_L t} - e^{-i\omega_L t}). \tag{16}$$

and E_{Laser} is the amplitude of the monochromatic laser operating at a drive frequency $\omega = \omega_L$. The reduced spectral response yields

$$\begin{aligned}
\frac{S(\omega = \omega_L)}{S(\omega = \omega_L)_{g=0}} &= \frac{\langle \tilde{b}_{ss}^\dagger \tilde{b}_{ss} \rangle}{\langle \tilde{b}_{ss}^\dagger \tilde{b}_{ss} \rangle_{g=0}} \\
&= \left(1 + \frac{\gamma_c}{\gamma_p} \frac{g^2}{(\omega_L - \omega_c^{NL})^2 + (\gamma_c/2)^2} \right) \left| \frac{q + \epsilon}{\epsilon + i} \right|^2.
\end{aligned} \tag{17}$$

The first term is the Fano profile, where $\epsilon = (\omega_L - \omega_{eff})/(\gamma_{eff}/2)$ and $q = (\omega_c^{NL} - i\gamma_c/2 - \omega_{eff})/(\gamma_{eff}/2)$; ϵ and q are the Fano parameters. The second

term is the Lorentz distribution due to the line-width broadening of the discrete state. The spectral distribution reduces to the Fano profile in the limit $\gamma_c \propto |V_a| \to 0$.

Since we are interested in single-photon blockade due to the Kerr-nonlinearity, $U \propto \chi_{eff}^{(3)}$, we calculate the second order correlation function $g_{ss}^{(2)}$ of light transmitted through the Kerr-cavity coupled to the driven broad-band emitter, at the steady state, as a function of U, i.e.,

$$
\begin{aligned}
g_{ss}^{(2)}(U) &\equiv \frac{\langle n_a, n_b| \, \tilde{a}_0^\dagger \, \tilde{a}_{ss}^\dagger(U) \tilde{a}_{ss}(U) \, \tilde{a}_0 \, |n_a, n_b\rangle}{(\langle \tilde{a}_0^\dagger \tilde{a}_0 \rangle)^2} \\
&= \frac{g^2}{n_a} \frac{\langle n_a - 1| \, E_{Laser}^2 \, |n_a - 1\rangle}{\left| \left(\omega_L - \omega_c^{NL}(U) + i\gamma_c/2\right)\left(\omega_L - \omega_p + i\gamma_p/2\right) - g^2 \right|^2}.
\end{aligned}
\tag{18}
$$

For single-photon blockade, the photon-number in the cavity is set to one, such that, $\omega_c^{NL}(U, N_c = 1) = \omega_c + U$. Importantly, the amplitude of the laser field to populate the bare $(N_c = 0)$ cavity mode with a single photon at steady state is such that

$$
\begin{aligned}
\langle n_a = 1| \, \tilde{a}_{ss}^\dagger \tilde{a}_{ss} \, |n_a = 1\rangle &= n_a = 1 \\
&= \frac{g^2 \, \langle n_a| \, E_{Laser}^2 \, |n_a\rangle}{\left| \left(\omega_L - \omega_c^{NL}(N_c = 0) + i\gamma_c/2\right)\left(\omega_L - \omega_p + i\gamma_p/2\right) - g^2 \right|^2}.
\end{aligned}
\tag{19}
$$

thus, it follows that

$$
\langle n_a| \, E_{Laser}^2 \, |n_a\rangle = n_a \left| (i\gamma_c/2)(\omega_c - \omega_p + i\gamma_p/2) - g^2 \right|^2 / g^2.
\tag{20}
$$

3   Previous work

Previous work focuses on individual cavities. [32] We design and characterize split ring resonator (SRR) cavities arranged in a dimer or trimer array. Due to the split of the ring, and the circular current path of the ring, these SRR cavities exhibit both electric and magnetic dipoles. We map out the electric g_E, magnetic g_H, and overall interaction strength $G = |g_E| \cos \phi - |g_B| \cos \theta$, and its effect on the normal mode energy splitting $G_{eff} = |G/\Omega_0|$, between coupled SRR dimers, as a function of the spatial degrees of freedom—exploring both the two-dimensional in-plane rotaion ϕ (Fig. 2, Table 1), and the three-dimensional out-of-plane tilt θ (Fig. 2, Table 2).
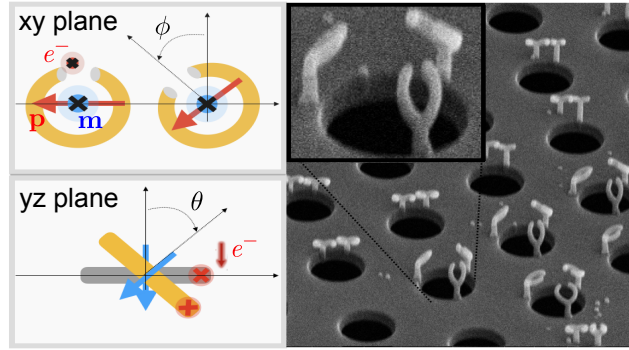

Figure 2: Graphical TOC: This work is currently under review at ACS Optical Applied Materials.

This study is the first to characterize the third-dimensional (3D) degree of freedom, where the analysis of the EEL probability shows that for a particular orientation, increasing the 3D tilt angle θ diminishes the magnetic coupling,

11

but enhances the overall light-matter interaction strength.

Table 1: 2D Parameter estimates

A $[\mathrm{s}^2 \cdot \mathrm{cm}^{-1}]$	$\hbar\omega_0$ [meV]	$\hbar|g_E|$ $[\mathrm{meV}^2]$	$\hbar|g_H|$ $[\mathrm{meV}^2]$
1.885×10^{-31}	359	6.5×10^{-2}	9.0×10^{-3}

ϕ [deg]	$\hbar\Omega_0$ [meV]	$\hbar\gamma_0$ [meV]	$\hbar|G_{\mathrm{eff}}|$ [meV]
0	362	47	65
45	360	47	54
90	359	47	25
135	365	55	64
180	370	58	82

Table 2: 3D Parameter estimates

ϕ [deg]	θ [deg]	$\hbar\Omega_0$ [meV]	$\hbar\gamma_0$ [meV]	$\hbar|G_{\mathrm{eff}}|$ [meV]	$\hbar\omega_0$ [meV]
0	0	389	52	33	410
0	15	387	51	85	$\sim$
90	0	390	78	20	$\sim$
90	15	404	48	15	$\sim$

Based upon the model provided in this work, we additionally examine the hybridization of individual 2D SRR trimers measured using EELS. Taken together, this study elucidates the geometric effects of 3D tilt on the SRR magnetic dipole moment and its role in the hybridization of coupled 3D SRRs, thus serving as a stepping stone for nano-engineering NIR metamaterials composed of coupled 3D SRR units. This work is currently under review at ACS Optical Applied Materials.

References

[1] Nicolas Gisin, Grégoire Ribordy, Wolfgang Tittel, and Hugo Zbinden. Quantum cryptography. *Reviews of modern physics*, 74(1):145, 2002.

[2] Charles H Bennett and Gilles Brassard. A quantum information science and technology roadmap. *Part*, 2:12, 2004.

[3] Charles H Bennett and Gilles Brassard. Proceedings of the ieee international conference on computers, systems and signal processing, 1984.

[4] Charles H Bennett. Quantum cryptography using any two nonorthogonal states. *Physical review letters*, 68(21):3121, 1992.

[5] Brahim Lounis and Michel Orrit. Single-photon sources. *Reports on Progress in Physics*, 68(5):1129, 2005.

[6] Matthew D Eisaman, Jingyun Fan, Alan Migdall, and Sergey V Polyakov. Invited review article: Single-photon sources and detectors. *Review of scientific instruments*, 82(7):071101, 2011.

[7] Andrew J Shields. Semiconductor quantum light sources. *Nature photonics*, 1(4):215–223, 2007.

[8] Stefan Strauf, Nick G Stoltz, Matthew T Rakher, Larry A Coldren, Pierre M Petroff, and Dirk Bouwmeester. High-frequency single-photon source with polarization control. *Nature photonics*, 1(12):704–708, 2007.

[9] Markus Hennrich, Thomas Legero, Axel Kuhn, and Gerhard Rempe. Photon statistics of a non-stationary periodically driven single-photon source. *New Journal of Physics*, 6(1):86, 2004.

[10] Tatjana Wilk, Simon C Webster, Axel Kuhn, and Gerhard Rempe. Single-atom single-photon quantum interface. *Science*, 317(5837):488–490, 2007.

[11] Christian Maurer, Christoph Becher, Carlos Russo, Jürgen Eschner, and Rainer Blatt. A single-photon source based on a single ca+ ion. *New journal of physics*, 6(1):94, 2004.

[12] Alfred B URen, Christine Silberhorn, Konrad Banaszek, and Ian A Walmsley. Efficient conditional preparation of high-fidelity single photon states for fiber-optic quantum networks. *Physical review letters*, 93(9):093601, 2004.

[13] Jay E Sharping, Marco Fiorentino, and Prem Kumar. Observation of twin-beam-type quantum correlation in optical fiber. *Optics letters*, 26(6):367–369, 2001.

[14] Elizabeth A Goldschmidt, Matthew D Eisaman, Jingyun Fan, Sergey V Polyakov, and Alan Migdall. Spectrally bright and broad fiber-based heralded single-photon source. *Physical Review A*, 78(1):013844, 2008.

[15] Feng Pan, Kevin C Smith, Hoang L Nguyen, Kassandra A Knapper, David J Masiello, and Randall H Goldsmith. Elucidating energy path-

ways through simultaneous measurement of absorption and transmission in a coupled plasmonic–photonic cavity. *Nano Letters*, 20(1):50–58, 2019.

[16] Fei Qin, Ye Liu, Zi-Ming Meng, and Zhi-Yuan Li. Design of kerr-effect sensitive microcavity in nonlinear photonic crystal slabs for all-optical switching. *Journal of Applied Physics*, 108(5):053108, 2010.

[17] Ye Liu, Fei Qin, Zhi-Yi Wei, Qing-Bo Meng, Dao-Zhong Zhang, and Zhi-Yuan Li. 10 fs ultrafast all-optical switching in polystyrene nonlinear photonic crystals. *Applied Physics Letters*, 95(13):131116, 2009.

[18] F Krausz, E Wintner, and G Leising. Optical third-harmonic generation in polyacetylene. *Physical Review B*, 39(6):3701, 1989.

[19] KS Wong, SG Han, and ZV Vardeny. Studies of resonant and preresonant femtosecond degenerate four-wave mixing in unoriented conducting polymers. *Journal of applied physics*, 70(3):1896–1898, 1991.

[20] SM Spillane, TJ Kippenberg, and KJ Vahala. Ultralow-threshold raman laser using a spherical dielectric microcavity. *Nature*, 415(6872):621–623, 2002.

[21] Kevin D Heylman and Randall H Goldsmith. Photothermal mapping and free-space laser tuning of toroidal optical microcavities. *Applied Physics Letters*, 103(21):211116, 2013.

[22] Salim Al-Kathiri, Wajdi Al-Khateeb, Mohd Hafizulfika, Mohamed Ridza Wahiddin, and Suhairi Saharudin. Characterization of mean photon number for key distribution system using faint laser. In *2008 International Conference on Computer and Communication Engineering*, pages 1237–1242. IEEE, 2008.

[23] Marlan O Scully and M Suhail Zubairy. Quantum optics, 1999.

[24] Claude Cohen Tannoudji, Gilbert Grynberg, and J Dupont-Roe. Atom-photon interactions, 1992.

[25] Daniel Finkelstein-Shapiro, Ines Urdaneta, Monica Calatayud, Osman Atabek, Vladimiro Mujica, and Arne Keller. Fano-liouville spectral signatures in open quantum systems. *Physical Review Letters*, 115(11):113006, 2015.

[26] Daniel Finkelstein-Shapiro, Monica Calatayud, Osman Atabek, Vladimiro Mujica, and Arne Keller. Nonlinear fano interferences in open quantum systems: An exactly solvable model. *Physical Review A*, 93(6):063414, 2016.

[27] Ugo Fano. Effects of configuration interaction on intensities and phase shifts. *Physical Review*, 124(6):1866, 1961.

[28] John David Jackson. Classical electrodynamics, 1999.

[29] Mark Hillery and Leonard D Mlodinow. Quantization of electrodynamics in nonlinear dielectric media. *Physical Review A*, 30(4):1860, 1984.

[30] Paul N Butcher and David Cotter. The elements of nonlinear optics, 1990.

[31] Niket Thakkar, Charles Cherqui, and David J Masiello. Quantum beats from entangled localized surface plasmons. *ACS Photonics*, 2(1):157–164, 2015.

[32] Grace Pakeltis, Zhongwei Hu, Austin G Nixon, Eva Mutunga, C Praise Anyanwu, Claire A West, Juan Carlos Idrobo, Harald Plank, David J Masiello, Jason D Fowlkes, et al. Focused electron beam induced deposition synthesis of 3d photonic and magnetic nanoresonators. *ACS Applied Nano Materials*, 2(12):8075–8082, 2019.